

Michelson Morley Experiment using Spherical Resonators

Michael E. Tobar, Senior *Member*, *IEEE*, James D. ANSTIE, and John G. HARTNETT

Abstract-- Spherical resonators are proposed for new highly sensitive Michelson-Morley experiments. Two modes with orthogonal propagation directions are identified for this purpose: 1. Whispering Gallery modes, which propagates like a ray along the equator of the sphere; 2. Whispering Longitude modes, which propagates as azimuthal wave fronts in the longitudinal direction. If the beat frequency between the modes is measured as the experiment is rotated, we show how to choose the axis of rotation in the laboratory frame to obtain maximum sensitivity to violations of Special Relativity.

Index Terms— Frequency Standards, Cavity Resonators, Special Relativity.

INTRODUCTION

THE most stable secondary frequency standards have been made from cylindrical cryogenically cooled sapphire and superconducting resonators[1-3]. Recently the SUPERconducting Microwave Oscillator (SUMO)[4] project has been proposed. This project considers placing two spatially orthogonal superconducting cylindrical resonators close together in one dewar to perform Michelson-Morley (MM)[5] and Kennedy-Thorndike (KT)[6] experiments on the International Space Station. In this work, we propose an alternative method using near degenerate “Whispering Spheroid” (WS) modes in a single spherical microwave resonator. In particular, we show that a mode exists, which can be classified as a “Whispering Longitude” (WL) mode, which propagates in an orthogonal direction to the well-known Whispering Gallery (WG) mode. Measuring the beat frequency between these two modes as they are rotated constitutes a MM experiment. Because the modes exist in the same cavity, significantly more common mode rejection of environmental influences can be expected.

The response to violations in Special Relativity (SR) has been calculated, which includes the way the experiment is rotated and the precession of the sidereal frame. We show how to rotate the experiment in the laboratory frame to obtain maximum sensitivity to violations in SR. Also, we propose the implementation of optimal filtering techniques. Long periods (1 to 2 years) of integration of the signal could easily be accommodated and significantly improve the signal to noise ratio. By changing the filter parameters a

search for the direction of the laboratory frame with respect to the supposed preferred frame may also be undertaken. Furthermore, this technique may be adapted to search for more general test theories of SR than previously proposed.

Experiments and calculation of mode properties for WS modes have been determined for spherical cavity resonators. We show that certain WS mode families have nearly an order of magnitude greater geometric factor than the modes used for the SUMO project. Thus, the utilization of these modes would also allow the added benefit of an order of magnitude increase of Q-factor.

ROBERTSON-MANSOURI-SEXL FRAMEWORK

Useful frameworks to test for violations in the Lorentz transforms have been developed by Robertson[7] and Mansouri and Sexl[8]. This framework describes a more general transformation between a moving frame S of velocity \underline{v} with respect to a preferred frame Σ (see fig. 1).

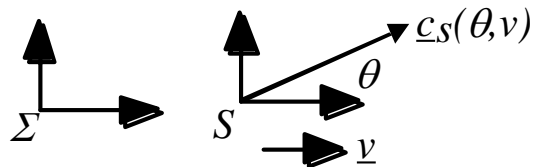


Fig. 1. Schematic of the moving frame, S , with respect to the preferred frame Σ .

The speed of light, c , is assumed to be constant in Σ and in general transforms to a non-constant value, $c_S(\theta, v)$, in S . In general $c_S(\theta, v)$ depends on the angle (θ) of light propagation with respect to the direction (\hat{v}) and magnitude (v) of \underline{v} . The fractional difference between c and $c_S(\theta, v)$ according to this transform is given by the Robertson-Mansouri-Sexl (RMS) equation below;

$$\chi(\theta, v) = \frac{c_S(\theta, v) - c}{c} = \chi_{MM}(v) \sin^2 \theta + \chi_{KT}(v) \quad (1)$$

$$\chi_{MM}(v) = \left(\frac{1}{2} - \beta + \delta \right) \left(\frac{v}{c} \right)^2, \text{ and } \chi_{KT}(v) = (\beta - \alpha - 1) \left(\frac{v}{c} \right)^2$$

Here, α is the time dilation parameter, β the length contraction parameter parallel to \underline{v} , and δ the length contraction parameter perpendicular to \underline{v} . Special Relativity is a subset of this transform with $\alpha = -1/2$, $\beta = 1/2$ and $\delta = 0$, in this case $\chi(\theta, v) = 0$. Current knowledge of these parameters comes from modern MM and KT experiments. The MM experiment tests the first term in (1) while the KT experiment tests the second term.

M. E. Tobar, J. D. Anstie and J. G. Hartnett are with the University of Western Australia, Crawley, WA 6009 Australia.

E-mail: mike@physics.uwa.edu.au

Web: <http://www.physics.uwa.edu.au/~mike/>

<http://www.fsm.physics.uwa.edu.au/>

MICHELSON-MORELY (MM) AND KENNEDY-THORNDIKE
(KT) EXPERIMENTS

The MM experiments test the first term in (1) by testing for length contractions in S that depend on the orientation of the light signal (θ). Modern experiments lock a microwave or laser oscillation to a high-Q resonator, with known mode structure and propagation[4, 9, 10]. The resonator is rotated and compared to a 90° orientated resonator-oscillator. Because of the $\text{Sin}^2(\theta)$ dependence, length contractions will occur at twice the frequency of the rotation. One problem with this type of MM experiment, is that the sensitivity to violations in SR depends on the orientation with respect to the supposed preferred frame. For example, in general there exists an alignment where the experiment is insensitive to violations of SR even if they exist. In this case, one must re-orientated the experiment to obtain maximum sensitivity, this requires a knowledge of the direction of \underline{v} . It is usual to assume that \underline{v} is the Earth's velocity with respect to the cosmic microwave background[11]. Corrections need to be made due to the change in sensitivity as the sidereal frame precesses in a 24-hour cycle. We show how our new experiment may be rotated in the laboratory frame with maximum sensitivity. However, the sensitivity still depends on the direction of \underline{v} and the precessing sidereal frame. In section 5 an expression is presented, which shows how the phase and amplitude of the signal varies as the direction with respect to the preferred frame changes. Because the form of the expected signal is known, it is possible to implement optimal filtering techniques to post-process the data and test for different directions of \underline{v} .

In general, the whole RMS equation is tested by a KT experiment. However, since the MM experiment involves a differential measurement, it can be made much more sensitively. Thus, the first term in the RMS equation is assumed zero. For example, a limit of $\chi_{MM}(v) < 3 \times 10^{-15}$ has been set using a Fabry-Perot interferometer[9]. In comparison a limit of $\chi_{KT}(v) < 2 \times 10^{-13}$ has been set by searching for sidereal shifts of a I_2 reference compared to a FP reference.

NATURE OF MODES IN A SPHERICAL RESONATOR

Separation of variables of Maxwell's Equations in spherical co-ordinates (ρ, θ, ϕ) leads to the solution of the radial field components[12] E_ρ and H_ρ . The mode solutions can be classified as Transverse Magnetic ($TM_{n\phi m}$) or Electric ($TE_{n\phi m}$) with respect to the radial direction, with the respective radial components of TM (2) and TE (1) modes given by;

$$E_\rho = n(n+1) \frac{\sqrt{k\rho}}{\rho^2} J_{n+\frac{1}{2}}(k\rho) P_n^m(\text{Cos}\theta) \frac{\text{Cos}(m\phi)}{\text{Sin}(m\phi)} \quad H_\rho = 0 \quad (2)$$

$$H_\rho = n(n+1) \frac{\sqrt{k\rho}}{\rho^2} J_{n+\frac{1}{2}}(k\rho) P_n^m(\text{Cos}\theta) \frac{\text{Cos}(m\phi)}{\text{Sin}(m\phi)} \quad E_\rho = 0 \quad (3)$$

Here n is the order of the spherical Bessel function, k is the wave number, m the number of 2π variations in the

azimuthal direction and p is the number of radial variations (which depends on k). The other field components ($H_\theta, H_\phi, E_\theta$ and E_ϕ) may be found from Maxwell's equations. The θ and ϕ terms for all field components are cyclic in 2π and are hence common to all spherical resonators with or without dielectric and cavity walls. Frequencies are determined by solving the boundary value problem in ρ , and thus depend on the dielectric and metallic boundaries. Tangential fields are matched at these boundaries to solve the problem. In the following analysis we use the example of an empty spherical cavity resonator of 5-cm diameter and compare the modes to the SUMO TM_{010} mode in a cylindrical resonator.

To create a stable frequency, a high-Q resonator is necessary. Superconducting resonators[2] with low surface resistance, R_s , have produced Q-factors as high as 10^{11} . The Q-factor is inversely proportional to R_s , the proportionality constant is known as the Geometric-factor, G , and is dependent on the mode geometry.

$$Q = G/R_s \quad (4)$$

The Geometric factor may be calculated from the ratio of the tangential H field at the conductor surface, to the H field in the volume of the resonator, and is given by;

$$G = \frac{\omega \iiint_V \mu_0 \bar{H}^* \cdot \bar{H} dV}{\iint_S \bar{H}_t^* \cdot \bar{H}_t ds} \quad (5)$$

Another important related parameter is the electric (P_{e_i}) and magnetic (P_{m_i}) filling factors, which represent the fraction of field energy to the total field energy, which is given by;

$$P_{e_i} = \frac{\iiint_V d|E_i|^2 dV}{\iiint_V \epsilon \underline{E}^* \cdot \underline{E} dV} \quad P_{m_i} = \frac{\iiint_V \mu |H_i|^2 dV}{\iiint_V \mu \underline{H}^* \cdot \underline{H} dV} \quad (6)$$

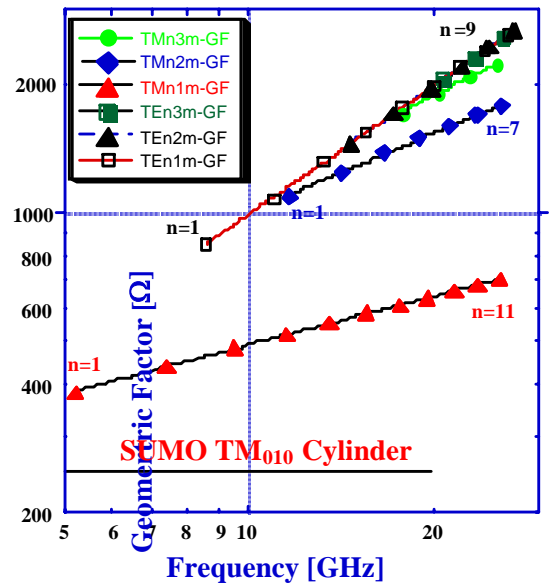


Fig. 2. Calculated Geometric factor versus frequency for a sphere of diameter 5-cm, compared to the TM_{010} mode in a cylinder of the same aspect ratio of SUMO. The diameter of the SUMO resonator fixes the

frequency at 8.6 GHz. Each point represents a degenerate mode family given by (2) and (3). If the sphere is perfect each member, $m = 0$ to n has the same frequency and Q-factor.

TABLE I
ELECTRIC AND MAGNETIC FILLING FACTORS FOR THE TE_{61m} MODES

m	Pe_θ	Pe_ϕ	Pm_ρ	Pm_θ	Pm_ϕ
6	0.926	0.074	0.992	0.001	0.008
5	0.749	0.251	0.992	0.002	0.006
4	0.556	0.444	0.993	0.003	0.004
3	0.361	0.639	0.993	0.005	0.003
2	0.185	0.815	0.993	0.006	0.001
1	0.055	0.945	0.992	0.007	0.000
0	0.000	1.000	0.991	0.009	0.000

where $i = \rho, \theta$ or ϕ . Fig. 2 compares the G of the SUMO resonator to modes in a spherical resonator and table 1 shows the filling factors for the TE_{61m} WS mode family. WS TE modes have most of the H-field in the H_ρ component and little in the tangential components, H_θ and H_ϕ . Thus, they have higher G than the TM modes, and a much larger G than the SUMO resonator. For example, the TE_{61m} mode has a geometric factor 8 time greater than the SUMO resonator. Fig. 2 also reveals that the G versus frequency for all TE modes is proportional to frequency with the same proportionality constant, independent of the mode numbers, n, p and m .

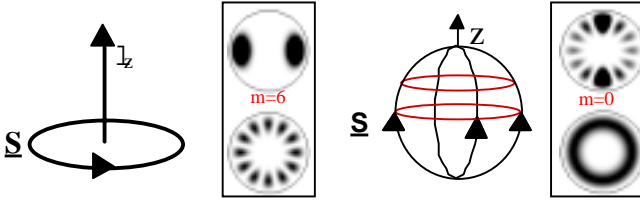


Fig. 3. Left, TE_{616} WG mode: Right, TE_{610} WL mode. The Poynting vector, \underline{S} , shows the direction of propagation on the sphere surface. The WG mode propagates like a ray around the equator with angular momentum in the z direction. The WL mode propagates as wave fronts along the longitude, which converges at the intersection with the z -axis. This results in a non-degenerate ($m = 0$) 'self' standing wave with maximum intensity along the z -axis. The density plots show $|H_\rho|^2$, above is in the z - y plane and below is in the x - y plane.

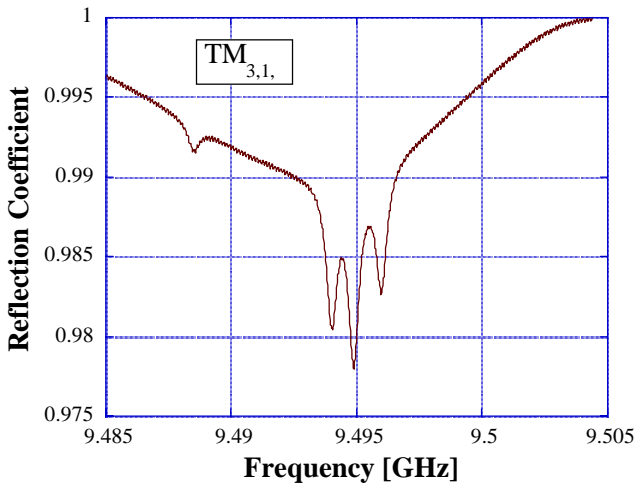


Fig. 4. Measure reflection coefficient for the TM_{31m} near-degenerate mode family.

From the filling factors (see table 1) it is straightforward

to deduce that WS modes propagate predominately around the spherical surface. Since $Pm_\rho \sim 1$ and $Pe_\rho = 0$, the cross product between \underline{E} and \underline{H} will give a Poynting vector (\underline{S}) with predominately S_θ and S_ϕ components. It is necessary to choose modes with orthogonal propagation for a MM experiment. For a given n , a set of degenerate WS modes exist, with $m = 0$ to n . In particular modes with $m = 0$, propagate along the longitudes, while the modes with $m = n$ propagate along the azimuth. A schematic showing \underline{S} and H_ρ is shown in figure 3. The other modes ($m = 1$ to $n-1$), propagate with a combination of directions. Experimentally we confirmed the presence of $n+1$ near degenerate modes for each n . For example, the TE_{31m} mode existed with 4-fold degeneracy with frequencies of 9.48851, 9.49399, 9.49488 and 9.49597 GHz, these compare well with the calculated value of 9.4919. The frequency separation is due to imperfections of the spherical surface. The reflection coefficient for this set of modes is shown in fig. 4.

SENSITIVITY TO TWO-WAY SPEED OF LIGHT ANISOTROPY

To determine the sensitivity of WL and WG modes to violations of SR, the average speed of light the modes sample must be calculated. First we assume the WG and WL modes share the same z -axis (this has been proven experimentally by the authors). The resonator axis (laboratory frame S) is labelled as z' and assumed to be at an angle θ_z to the preferred frame (direction of \underline{y} (z) in the absolute frame Σ).

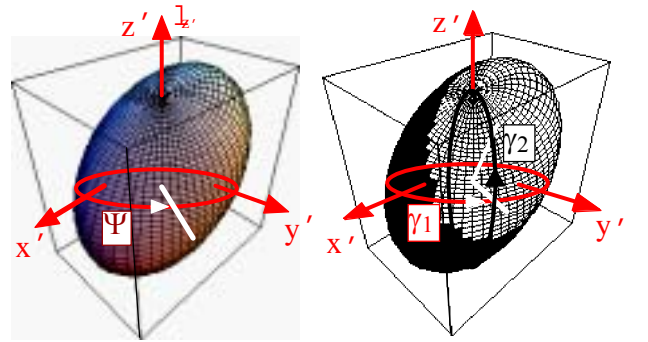


Fig. 5. Speed of light ellipsoid given by (1) rotated with respect to the WS resonator frame.

Eq. (1) is an ellipsoid and must be calculated in the rotated frame, a schematic 3-D plot of (1) in the rotated frame is shown in fig. 5. To calculate the average speed of light the integrals in (7) and (8) are performed in the resonator frame as shown fig. 5 (details of the calculation are not presented here, and may be obtained from the authors).

$$\chi(\theta_z, \nu)_{av}|_{WG} = \frac{1}{\pi} \int_0^\pi \left(\frac{c(\theta_z, \psi + \pi/2, \nu)}{c} - 1 \right) d\psi = \chi_{MM}(\nu) \left(\frac{1 + \cos^2 \theta_z}{2} \right) \quad (7)$$

$$\chi(\theta_z, \nu)_{av}|_{WL} = \frac{1}{\pi} \int_0^\pi \left(\frac{1}{\pi} \int_0^\pi \left(\frac{c(\theta_z, \gamma_1, \gamma_2 + \pi/2, \nu)}{c} - 1 \right) d\gamma_2 \right) d\gamma_1 = \chi_{MM}(\nu) \left(\frac{2 + \sin^2 \theta_z}{4} \right) \quad (8)$$

The beat frequency between the WL and WG modes will be given by the difference between (7) and (8), and is thus of the form:

$$\frac{\Delta f_{WG-WL}}{f} = \frac{1}{4} \chi_{MM}(\nu) \left(2 \cos^2 \theta_z - \sin^2 \theta_z \right) \quad (9)$$

Because the modes have different propagation and share the same z-axis, (9) is only dependent on θ_z . For standard MM experiments this expression depends on two angles of rotation with respect to the absolute frame rather than the position of the z' -axis. This is because the standard experiments use two of the same modes orientated at 90° . (The author has verified this in the case of two 90° orientated WG mode and SUMO type resonators). Consequently, if we spin the resonator around its z-axis on time scales faster than the rotation of the earth, then the experiment will be insensitive to violations in SR even if they exist, as θ_z does not change. To obtain maximum sensitivity, the resonator must be spun around the axis perpendicular to z' . Even though we have determined the way to rotate the experiment, the sensitivity will still depend on the initial angle, θ_i between z and z' at $t = 0$, as well as the direction of rotation, λ , as shown in fig. 6.

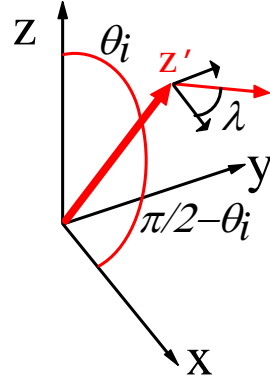


Fig. 6. In a MM experiment the z-axis of the WL and WG modes (z' vector shown) is rotated with respect to the absolute frame. The rotation may be defined by two angles, θ_i and λ . Here θ_i is the initial angle between the z- and z' -axis (at $t = 0$), and λ defines the direction of the rotating vector with respect to the x-axis. The position of the x-axis is defined as the direction of the projection of z' in the plane perpendicular to z , at $t = 0$.

By applying the relevant rotational co-ordinate transforms, if the resonator is rotated at ω rads/s, then the beat signal is at 2ω , and from (9) this can be shown to be of the form.

$$\frac{\Delta f_{WG-WL}}{f} = \frac{3}{8} \chi_{MM}(\nu) \left(1 - \sin^2 \theta_i \sin^2 \lambda \right) \cos[2\omega t + \vartheta(\theta_i, \lambda)] \quad (10)$$

Thus, violations in SR will manifest as a 2ω variation of the beat frequency. Also, the amplitude and phase will be modulated due to the precession of the earth's sidereal frame, which must be taken into account when performing the search. The known form of the expected signal may be used to our advantage in the post-processing of the data. Optimal filter techniques may be used to search for a signal of known characteristic amongst the noise. In general there are three unknown parameters we must determine during our search for violations in SR, ie ν , θ_i and λ . These three parameters will vary due to the rotation of the sidereal

frame. The first term, $\chi_{MM}(\nu)$, will cause an amplitude modulation at the sidereal frequency in a similar way to a KT experiment, while the θ_i and λ dependent terms will cause amplitude and phase modulation at twice the sidereal frequency. This technique may be extended to search for more complicated violations in SR, i.e. biaxial symmetric violation (This response has been calculated by the authors). This could occur if the supposed length contraction parameter perpendicular to \underline{v} , δ , had a preferred direction itself, i.e. it is a function of the azimuth angle (ϕ) in the plane perpendicular to the motion. A different optimal filter template may be applied to the same data to undergo a new search for biaxial violations. If there does exist violations in SR, it is important that the phase and amplitude variations assumed are correct, otherwise the effective integration (or filtering) of the signal may not increase the signal as expected and hence the upper limits to violations in SR cited may not be correct. This is specially important as the time for integrating the signal is increased.

We propose to perform a MM experiment with spherical resonators made from superconducting niobium or sapphire monocrystal. Implementing resonators based on these materials has produced highly stable microwave oscillators, which exhibit frequency instabilities of order 1 part in 10^{16} at short time intervals of order 1 to 100 seconds[1, 2]. Some gain with respect to data analysis could be expected by placing two spherical resonators in the same cryogenic dewar, with one orientated to attain maximum sensitivity (system A) and the other to obtain zero (system B). This will enable two simultaneous MM experiments. Each system will be operated in dual mode configuration that will simultaneously excite the WL and WG modes. The dual-mode technique has been developed independently as a new method to attain frequency stability in an anisotropic system[13], and will be straightforward to adapt to this situation. Each system will be analysed for signals according to (5). Signals from both systems may be compared. If a violation in SR is observed one would expect a stronger signal from the A system. System B may be used as a check for systematic and statistical errors.

CONCLUSION

If a spherical sapphire or superconducting oscillator is realised with state of the art frequency instability of 10^{-16} , it is not unreasonable to assume that a differential measurement could measure $\chi_{MM}(\theta, \nu) \sim 10^{-17}$, which would be greater than two orders of magnitude improvement in the MM experiment. Also, by utilising the optimal filter technique the sensitivity may be further improved by integration over long periods. A variety of test theories as well as the direction of a preferred axis may be tested for, by simply post-processing the data.

ACKNOWLEDGMENT

This work was supported by the Australian Research Council.

REFERENCES

- [1] S. Chang, A. Mann, and A. Luiten, "improved cryogenic sapphire oscillator with exceptionally high frequency stability," *Electron. Lett.*, vol. 36, pp. 480-481, 2000.
- [2] S. R. Stein and J. P. Turneaure, "Superconducting-cavity stabilized oscillators with improved frequency stability," *Proc. of IEEE*, vol. 36, pp. 1245, 1975.
- [3] G. J. Dick, R. T. Wang, and R. T. Tjoelker, "Cryo-cooled sapphire oscillator with ultra-high stability," *Proc. IEEE Int. Freq. Contr. Symp.*, vol. 52, pp. 528-533, 1998.
- [4] S. Buchman, M. Dong, W. Moeur, S. Wang, J. A. Lipka, and J. P. Turneaure, "A space-based superconducting microwave oscillator clock," *Adv. Space Res.*, vol. 25, pp. 1251-1254, 2000.
- [5] A. A. Michelson and E. W. Morley, *Am. J. Sci.*, vol. 34, pp. 333, 1887.
- [6] J. J. Kennedy and E. M. Thorndike, *Phys. Rev. B*, vol. 42, pp. 400, 1932.
- [7] H. P. Robertson, *Rev. Mod. Phys.*, vol. 21, pp. 378, 1949.
- [8] R. Mansouri and R. U. Sexl, "A test theory of relativity: I. Simultaneity and clock synchronization," *Gen. Relativ. Gravit.*, vol. 8, pp. 497-514, 1977.
- [9] A. Brilliet and J. L. Hall, "Improved laser test of the isotropy of space," *Phys. Rev. Lett.*, vol. 42, pp. 549-552, 1979.
- [10] C. Lammerzahl, H. Dittus, A. Peters, and S. Schiller, "OPTIS: a satellite-based test of special and general relativity," *Class. Quantum Grav.*, vol. 18, pp. 2499-2508, 2001.
- [11] G. F. Smoot, M. V. Gorenstein, and R. A. Muller, *Phys. Rev. Lett.*, vol. 39, pp. 898, 1977.
- [12] J. A. Stratton, *Electromagnetic Theory*. New York: McGraw-Hill, 1941.
- [13] M. E. Tobar, E. N. Ivanov, J. G. Hartnett, and C. R. Locke, "Novel temperature control of a sapphire loaded cavity oscillator from the difference frequency of WGE and WGH modes," in *Proc. 2001 IEEE Int. Freq. Contr. Symp.*, 2001.